

LETTER TO THE EDITOR

# Water production in comet 81P/Wild 2 as determined by *Herschel*/HIFI<sup>★</sup>

M. de Val-Borro<sup>1</sup>, P. Hartogh<sup>1</sup>, J. Crovisier<sup>2</sup>, D. Bockelée-Morvan<sup>2</sup>, N. Biver<sup>2</sup>, D. C. Lis<sup>3</sup>, R. Moreno<sup>2</sup>, C. Jarchow<sup>1</sup>, M. Rengel<sup>1</sup>, S. Szutowicz<sup>4</sup>, M. Banaszekiewicz<sup>4</sup>, F. Bensch<sup>5</sup>, M. I. Błęcka<sup>4</sup>, M. Emprechtinger<sup>3</sup>, T. Encrenaz<sup>2</sup>, E. Jehin<sup>6</sup>, M. Küppers<sup>7</sup>, L.-M. Lara<sup>8</sup>, E. Lellouch<sup>2</sup>, B. M. Swinyard<sup>9</sup>, B. Vandenbussche<sup>10</sup>, E. A. Bergin<sup>11</sup>, G. A. Blake<sup>3</sup>, J. A. D. L. Blommaert<sup>10</sup>, J. Cernicharo<sup>12</sup>, L. Decin<sup>10,13</sup>, P. Encrenaz<sup>14</sup>, T. de Graauw<sup>15,16,17</sup>, D. Hutsemékers<sup>6</sup>, M. Kidger<sup>18</sup>, J. Manfroid<sup>6</sup>, A. S. Medvedev<sup>1</sup>, D. A. Naylor<sup>19</sup>, R. Schieder<sup>20</sup>, D. Stam<sup>15</sup>, N. Thomas<sup>21</sup>, C. Waelkens<sup>10</sup>, R. Szczerba<sup>22</sup>, P. Saraceno<sup>23</sup>, A. M. Di Giorgio<sup>23</sup>, S. Philipp<sup>24</sup>, T. Klein<sup>24</sup>, V. Ossenkopf<sup>20,15</sup>, P. Zaal<sup>15</sup>, and R. Shipman<sup>15</sup>

(Affiliations can be found after the references)

Received May 31, 2010; accepted

## ABSTRACT

The high spectral resolution and sensitivity of *Herschel*/HIFI allows for the detection of multiple rotational water lines and accurate determinations of water production rates in comets. In this letter we present HIFI observations of the fundamental  $1_{10}-1_{01}$  (557 GHz) ortho and  $1_{11}-0_{00}$  (1113 GHz) para rotational transitions of water in comet 81P/Wild 2 acquired in February 2010. We mapped the extent of the water line emission with five point scans. Line profiles are computed using excitation models which include excitation by collisions with electrons and neutrals and solar infrared radiation. We derive a mean water production rate of  $1.0 \times 10^{28}$  molecules  $s^{-1}$  at a heliocentric distance of 1.61 AU about 20 days before perihelion, in agreement with production rates measured from the ground using observations of the 18-cm OH lines. Furthermore, we constrain the electron density profile and gas kinetic temperature, and estimate the coma expansion velocity by fitting the water line shapes.

**Key words.** Comets: individual: 81P/Wild 2 – molecular processes – radiative transfer – submillimetre – techniques: spectroscopic

## 1. Introduction

Water is the main volatile constituent of cometary comae. Thus it is crucial to determine the water production rate to understand cometary activity and determine the relative abundances of other volatiles in the coma (see e.g. Bockelée-Morvan 1987). Water molecules in cometary atmospheres are excited by collisions with neutrals and electrons, and radiative pumping of the fundamental vibrational levels by the solar infrared radiation. The fundamental  $1_{10}-1_{01}$  ortho-water transition at 556.936 GHz is one of the strongest lines in cometary spectra. This transition has been detected using the Submillimeter Wave Astronomical Satellite (SWAS) (Neufeld et al. 2000), and subsequently with Odin (Lecacheux et al. 2003; Biver et al. 2007, 2009) and the *Herschel* Space Observatory (Hartogh et al. 2010). *Herschel* provided the first detection of the  $2_{12}-1_{01}$  (1669.905 GHz) ortho and  $1_{11}-0_{00}$  (1113.343 GHz) para transitions of water in cometary atmospheres (Hartogh et al. 2010). The continuum emission in comet C/2006 W3 (Christensen) has been measured by *Herschel* (Bockelée-Morvan et al. 2010).

Comet 81P/Wild 2 is a Jupiter family comet that was the target of NASA's *Stardust* sample return mission (Brownlee et al. 2004). Thousands of particles in the submillimeter size range were collected for laboratory study during the *Stardust* flyby on January 2, 2004 (Brownlee et al. 2006). Optical images of the nucleus obtained by the navigation camera show very com-

plex topographic features (Brownlee et al. 2004). Gas production rates for several molecules have been monitored at multiple apparitions (Osip et al. 1992; Mäkinen et al. 2001; Fink et al. 1999; Farnham & Schleicher 2005). A maximum water production rate of  $Q_{H_2O} \sim 1.1 \times 10^{28} s^{-1}$  is estimated from narrowband photometry of OH emission in the near-UV (Farnham & Schleicher 2005).

The Heterodyne Instrument for the Far-Infrared (HIFI) on-board *Herschel* is well suited to observe water vapor in cometary coma with high spectral resolution (de Graauw et al. 2010; Pilbratt et al. 2010). Comet 81P/Wild 2 was observed with HIFI on February 1–4, 2010, in the framework of the *Herschel* guaranteed time key project “Water and related chemistry in the Solar System” (Hartogh et al. 2009).

## 2. HIFI observations

Comet 81P/Wild 2 passed its perihelion on February 22.7 UT at  $r_h = 1.5981$  AU from the Sun. The *Herschel* observations took place in early February about 20 days before perihelion, at heliocentric distance  $r_h \approx 1.6$  AU and a distance of  $\Delta \approx 0.9$  AU from *Herschel*. The comet could not be observed after February 14 due to visibility constraints. HIFI can observe two polarizations simultaneously. With a spectral resolution of 1.1 MHz (Wide Band Spectrometer; WBS) or 140 KHz (High Resolution Spectrometer; HRS) HIFI can resolve spectrally cometary line shapes and asymmetries (Hartogh et al. 2010).

Table 1 shows a summary of the HIFI observations of the  $1_{10}-1_{01}$  (557 GHz, HIFI bands 1a and 1b) and  $1_{11}-0_{00}$  (1113

<sup>★</sup> *Herschel* is an ESA space observatory with science instruments provided by European-led Principal Investigator consortia and with important participation from NASA.

GHz, HIFI band 4b) water lines in comet 81P/Wild 2. The position of the comet and its relative motion with respect to *Herschel* were calculated using the JPL's HORIZONS system. The *Herschel* telescope has a diameter of 3.5 m, with the corresponding HIFI Half Power Beam Widths (HPBW) of 19.2'' and 38.1'' at 1113, and 557 GHz, respectively. The corresponding beam sizes projected on the comet are  $1.5$  and  $2.2 \times 10^4$  km, respectively. Observations were conducted in the standard dual beam switch (DBS) cross map observing mode with a chopper speed of 4 Hz and a separation of the cross positions corresponding to a Nyquist sampling of the beam size (22'', 19'', and 10'' for observations in bands 1a, 1b, and 4b, respectively). One axis of the cross was aligned along the Sun direction at PA = 111°. The reference OFF position was 3' from the position of the comet. This observing mode was not released at the time of the observations.

### 3. Data analysis

#### 3.1. Water line emission

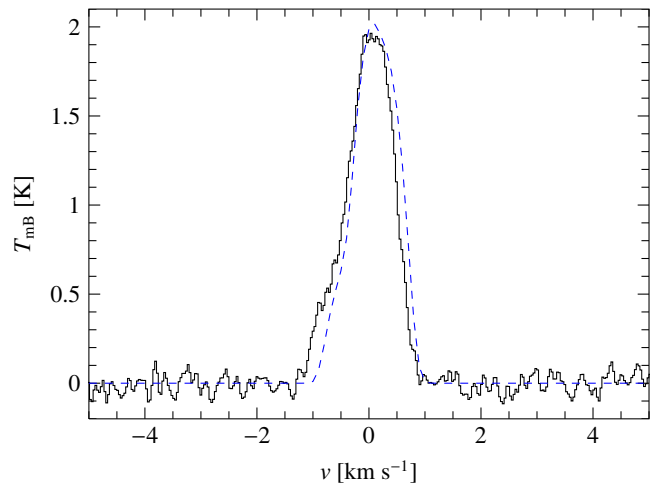
The data were reduced to the level 2 products using the standard *Herschel* Interactive Processing Environment (HIPE) 3.0 pipeline for HIFI (de Graauw et al. 2010). Integrated line intensities and velocity offsets in the comet rest frame are given in Table 1 for the central point in the maps. Line intensities are calculated from the weighted averages of spectra in horizontal (H) and vertical (V) polarizations. We scaled the main beam brightness temperature using the beam efficiency of the *Herschel* telescope of 0.7 and 0.75 for the 1113 and 557 GHz lines respectively (see e.g. Hartogh et al. 2010). The uncertainties in line intensity, velocity shift and water production rates are 1- $\sigma$  statistical uncertainties. Uncertainties in the sideband gain ratio, which reach 5% (Roelfsema et al. 2010), are considered in the data analysis.

Figure 1 shows the HRS spectrum of the  $1_{10}-1_{01}$  ortho-water line at 557 GHz observed on February 4.24 UT at the center of the map. The central spectrum of the map of the  $1_{11}-0_{00}$  para-water line at 1113 GHz, averaging the two observations to increase the signal-to-noise ratio, is shown in Fig. 2. These spectra are uniformly weighted averages of the H and V polarizations. They correspond also to the average of the central points of the horizontal and vertical drifts of the cross map. The frequency scale of the observed spectra was corrected for the geocentric velocity of the comet and the spacecraft orbital velocity. The lines are optically thick and slightly asymmetric due to self-absorption effects in the foreground coma. We estimate a mean expansion velocity  $v_{\text{exp}} = 0.6 \text{ km s}^{-1}$  from the width of the 557 GHz line (Biver et al. 2007). Expansion velocities in the range  $v_{\text{exp}} = 0.5 - 0.8 \text{ km s}^{-1}$  are typical for weak comets.

Mapping observations at 557 and 1113 GHz are shown in Figs. 3 and 4, and *online* Fig. 5.

#### 3.2. Radiative transfer modelling

Molecular excitation in the outer coma is dominated by collisions with electrons and infrared fluorescence by solar radiation. We use a spherically symmetric Monte Carlo radiative transfer numerical code to compute the populations of the water rotational levels as function of the distance from the nucleus (see Hartogh et al. 2010, and references therein). A constant gas temperature of  $T = 40 \text{ K}$  is assumed. The ortho-to-para water ratio in comets varies from 2.5 to 3 (e.g. Bonev et al. 2007, and references therein). We assume a value of 3. The scaling factor of



**Fig. 1.** Central point in the DBS map of the ortho-water line at 556.936 GHz in comet 81P/Wild 2 obtained by the HRS on February 4.24 UT. The velocity scale is given with respect to the comet rest frame with a resolution of  $\sim 32 \text{ m s}^{-1}$ . A synthetic line profile for isotropic outgassing with  $v_{\text{exp}} = 0.6 \text{ km s}^{-1}$ ,  $T = 40 \text{ K}$ , and  $x_{n_e} = 0.2$  is shown by the dashed line.

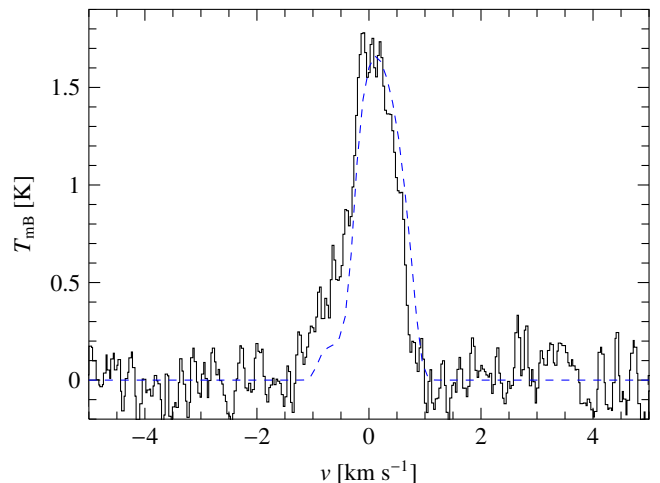


**Fig. 2.** Average of the HRS observations of the para-water line at 1113.343 GHz towards the nucleus of comet 81P/Wild 2 obtained on February 2.13 UT and 2.15 UT. The velocity resolution is  $\sim 32 \text{ m s}^{-1}$  after smoothing. The dashed line shows the best fit profile for the same parameters as in Fig. 1.

the electron density profile with respect to a nominal profile deduced from 1P/Halley *in situ* data is chosen to be  $x_{n_e} = 0.2$  and 1. The former value was found to best explain the brightness distribution of the  $1_{10}-1_{01}$  line obtained from mapping observations (Biver et al. 2007; Hartogh et al. 2010).

The radiative transfer equation is solved along different lines of sight through the coma covering  $2.5 \times \text{HPBW}$ , and the beam averaged emission spectra are computed. We obtain the water production rate by comparing the calculated and observed line intensities. The synthetic line profiles agree approximately with the observed line shapes (Figs. 1–2). The differences (overall shift and excess emission in the blue wing of the profiles) suggest preferential outgassing towards the Sun and a day/night asymmetry in the gas velocity field.

**Table 1.** HIFI observations of water vapour in comet 81P/Wild 2 and derived water production rates. The observations were acquired in February 2010 using the standard fast DBS cross map observing mode. The intensity, velocity shift and  $Q_{\text{H}_2\text{O}}$  correspond to the average of the central points in the cross maps.

Obs. ID	UT start date [mm/dd.ddd]	$\Delta$ [AU]	$r_h$ [AU]	Band	Frequency [GHz]	Integration time [s]	Intensity [K km s <sup>-1</sup> ]	Velocity shift [m s <sup>-1</sup> ]	$Q_{\text{H}_2\text{O}}^a$ [10 <sup>28</sup> s <sup>-1</sup> ]
1342190098	02/1.443	0.949	1.612	1a	556.9360	684	1.807 ± 0.012	4 ± 5	1.00 ± 0.05
1342190185	02/4.235	0.927	1.609	1b	556.9360	748	2.077 ± 0.015	-10 ± 5	1.13 ± 0.06
1342190231	02/2.134	0.943	1.611	4b	1113.3430	390	1.997 ± 0.053	-58 ± 21	1.07 ± 0.06
1342190232	02/2.151	0.943	1.611	4b	1113.3430	366	1.594 ± 0.052	-41 ± 26	0.86 ± 0.05

<sup>(a)</sup> Water production rates computed with  $T = 40$  K and  $x_{n_e} = 0.2$ . The error bar includes a 5% calibration uncertainty in the sideband gain ratio.

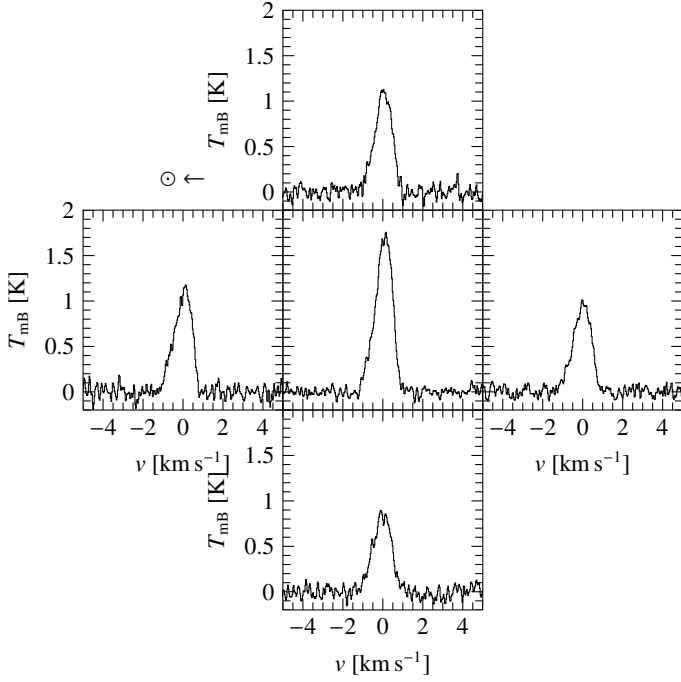


**Fig. 3.** DBS cross-map of the ortho-water  $1_{10}-1_{01}$  transition obtained with the HRS on February 1.44 UT. Offset positions are  $\sim 22''$  apart. The velocity resolution is  $\sim 32$  m s<sup>-1</sup>. The Sun direction is indicated.

### 3.3. Water production rates

Mapping observations can be used to constrain excitation parameters such as the neutral gas kinetic temperature and electron density scaling factor. The spacing of  $10''$  and  $22''$  between the observed positions corresponds to distances of  $\sim 1.2 \times 10^4$  and  $2.4 \times 10^4$  km at the distance of the comet, respectively, where the excitation of the water rotational levels is controlled both by collisions with electrons and infrared fluorescence (see Fig. 5 in Hartogh et al. 2010). Figure 6 shows the evolution of the line area of the 557 and 1113 GHz lines as a function of the position offset. As shown in Fig. 6, model calculations performed with  $T = 40$  K and  $x_{n_e} = 0.2$  provide a satisfactory fit to the observed radial brightness profiles. For a larger electron content ( $x_{n_e} = 1$ ), the line intensities at the offset positions are lower than observed. Production rates for  $x_{n_e} = 0.2$  are consistent with values obtained from OH observations (Crovisier et al. in preparation), while those for  $x_{n_e} = 1$  are about a factor of two lower.

The water production rates derived from the 557 and 1113 GHz lines are consistent with each other and in the range  $0.9-1.1 \times 10^{28}$  s<sup>-1</sup>. Model calculations show that the  $I(557 \text{ GHz})/I(1113 \text{ GHz})$  intensity ratio does not depend strongly on

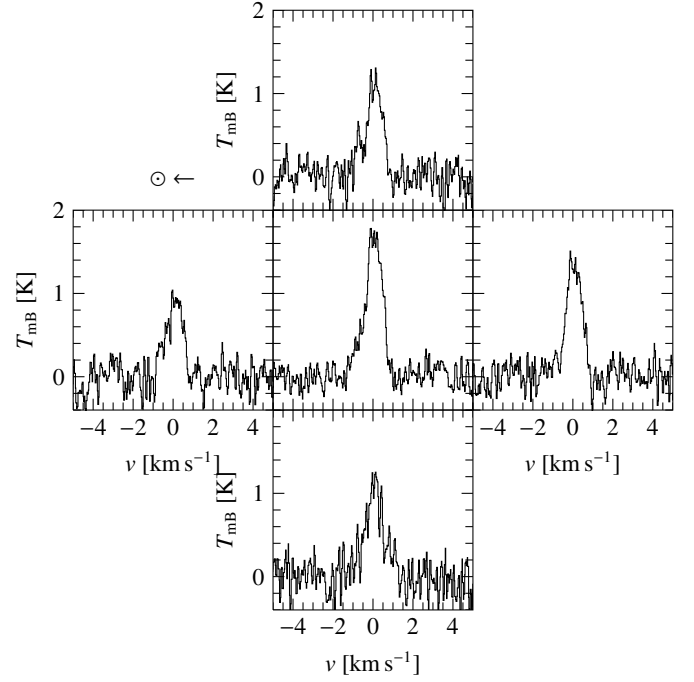


**Fig. 4.** Average of the cross-maps of the  $1_{11}-0_{00}$  para-water line obtained with the HRS on February 2.13 and 2.15 UT. The offset spacing is  $\sim 10''$  and the effective velocity resolution after smoothing is  $\sim 32$  m s<sup>-1</sup>. The Sun direction is indicated.

the  $x_{n_e}$  parameter. Gas kinetic temperatures  $T$  in the range 30–50 K provide a satisfactory fit of the measured intensity ratio, averaging the lines observed at the different dates and considering uncertainties in flux calibration. Lower temperatures (by  $\sim 15$  K) are retrieved when the ortho-to-para ratio is taken equal to 2.5. Such low  $T$  values are typical for comets of relatively low activity. However, these temperature retrievals are possibly affected by the non-simultaneity of the observations.

### 3.4. Comparison with observations of water photodissociation products

In support of the *Herschel* observations, the OH lines at 18-cm were observed with the Nançay radio telescope from November 16, 2009 to February 14, 2010 (Crovisier et al. in preparation). The methods of observation and analysis are described in Crovisier et al. (2002). The comet could be detected only after integrating over many days in December and January. It could not be detected close to perihelion because the OH maser inversion was small at that time. Water is the only significant parent molecule of the OH radical in cometary atmospheres and

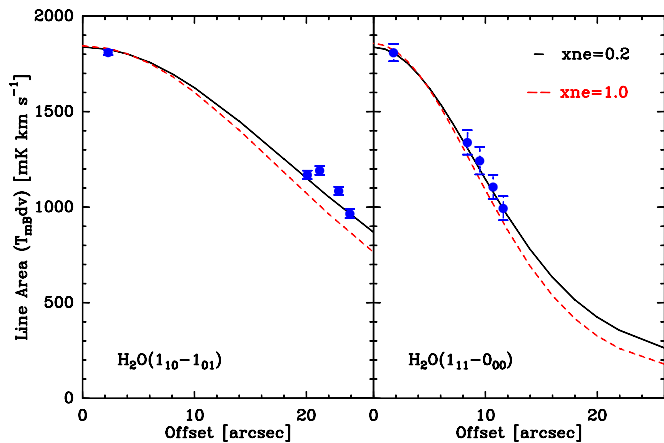


**Fig. 6.** Intensities of the  $1_{10}-1_{01}$  (Feb. 1.44 UT, left panel) and  $1_{11}-0_{00}$  (Feb. 2.13-2.15 UT, right panel) lines as a function of position offset from the estimated position of the peak brightness. Model calculations for  $x_{ne} = 0.2$  and  $1$  are shown with a black solid line and red dashed line, respectively. We assumed  $T = 40$  K and  $v_{exp} = 0.6$  km s $^{-1}$ .

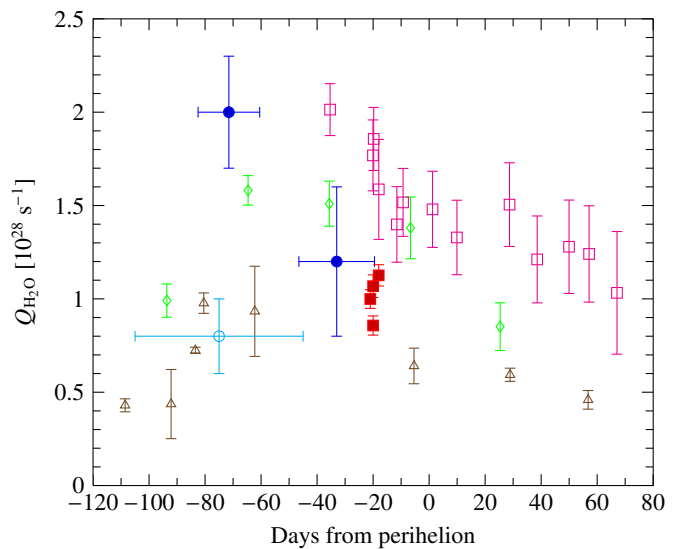
the lifetimes of the two species are well known, allowing for a determination of the water production rate (see e.g. Cochran & Schleicher 1993). The retrieved water production rates, including the HIFI retrievals, are shown in Fig. 7.

Figure 7 includes water production rates measured for the 1997 apparitions from OH narrowband photometry (Farnham & Schleicher 2005), spectroscopy of the  $^1\text{D}$  line of atomic oxygen (Fink et al. 1999) and Lyman- $\alpha$  measurements made with the SWAN instrument onboard SOHO (Mäkinen et al. 2001). The latter water production rates are about a factor of two higher than those obtained from narrowband photometry of OH emission (Farnham & Schleicher 2005). The higher production rates measured 80–20 days before perihelion may indicate a seasonal effect, with a water production rate peak at  $\sim 40$ –60 days pre-perihelion (see e.g. Szutowicz et al. 2008).

#### 4. Conclusions

Although comet 81P/Wild 2 has been extensively observed from the ground, it is still poorly observed at sub-millimeter wavelengths. 81P/Wild 2 was observed with HIFI in the period 1-4 February 2010 at 1.6 AU heliocentric distance and 0.95 AU from *Herschel*. The fundamental ortho- and para-water rotational transitions at 556.936 GHz and 1113.343 GHz were detected at high spectral resolution. DBS cross-maps were obtained to study the excitation conditions throughout the coma. We calculate a water production rate in the range  $0.9$ – $1.1 \times 10^{28}$  s $^{-1}$  using a radiative transfer code which includes collisional effects and infrared fluorescence by solar radiation. Water production rates are in good agreement with those derived from ground-based observations of the OH 18-cm emission at the Nançay radio telescope about 30 days before perihelion.

*Acknowledgements.* HIFI has been designed and built by a consortium of institutes and university departments from across Europe, Canada and the United States under the leadership of SRON Netherlands Institute for Space Research, Groningen, The Netherlands and with major contributions from Germany, France and the US. Consortium members are: Canada: CSA, U.Waterloo; France: CESR, LAB, LERMA, IRAM; Germany: KOSMA, MPIfR, MPS; Ireland, NUI Maynooth; Italy: ASI, IFSI-INAF, Osservatorio



**Fig. 7.** Water production rates with  $1$ - $\sigma$  uncertainties in comet 81P/Wild 2 as a function of time from perihelion. HIFI measurements are shown by squares. Filled circles represent OH 18-cm line observations with the Nançay radio telescope. Water production rates for the 1997 apparition from Crovisier et al. (2002), Farnham & Schleicher (2005), Fink et al. (1999) and Mäkinen et al. (2001) are shown by empty circles, triangles, diamonds and squares, respectively.

Astrofisico di Arcetri-INAF; Netherlands: SRON, TUD; Poland: CAMK, CBK; Spain: Observatorio Astronómico Nacional (IGN), Centro de Astrobiología (CSIC-INTA). Sweden: Chalmers University of Technology - MC2, RSS & GARD, Onsala Space Observatory, Swedish National Space Board, Stockholm University - Stockholm Observatory; Switzerland: ETH Zürich, FHNW; USA: Caltech, JPL, NHSC. HIPE is a joint development by the *Herschel* Science Ground Segment Consortium, consisting of ESA, the NASA *Herschel* Science Center, and the HIFI, PACS and SPIRE consortia. This development has been supported by national funding agencies: CEA, CNES, CNRS (France); ASI (Italy); DLR (Germany). Additional funding support for some instrument activities has been provided by ESA. Support for this work was provided by NASA through an award issued by JPL/Caltech. DCL is supported by the NSF, award AST-0540882 to the Caltech Submillimeter Observatory. SS, MB and MIB are supported by the Polish Ministry of Education and Science (MNiSW).

#### References

- Biver, N., Bockelée-Morvan, D., Colom, P., et al. 2009, *A&A*, 501, 359  
Biver, N., Bockelée-Morvan, D., Crovisier, J., et al. 2007, *Planet. Space Sci.*, 55, 1058  
Bockelée-Morvan, D. 1987, *A&A*, 181, 169  
Bockelée-Morvan, D., Hartogh, P., Crovisier, J., et al. 2010, *A&A* in press  
Bonev, B. P., Mumma, M. J., Villanueva, G. L., et al. 2007, *ApJ*, 661, L97  
Brownlee, D. E., Horz, F., Newburn, R. L., et al. 2004, *Science*, 304, 1764  
Brownlee, D. E., Tsou, P., Aléon, J., et al. 2006, *Science*, 314, 1711  
Cochran, A. L. & Schleicher, D. G. 1993, *Icarus*, 105, 235  
Crovisier, J., Colom, P., Gérard, E., Bockelée-Morvan, D., & Bourgois, G. 2002, *A&A*, 393, 1053  
de Graauw, Th., Helmich, F. P., Philipps, T. G., et al. 2010, *A&A* in press  
Farnham, T. L. & Schleicher, D. G. 2005, *Icarus*, 173, 533  
Fink, U., Hicks, M. P., & Fevig, R. A. 1999, *Icarus*, 141, 331  
Hartogh, P., Crovisier, J., de Val-Borro, M., et al. 2010, *A&A* in press  
Hartogh, P., Lellouch, E., Crovisier, J., et al. 2009, *Planet. Space Sci.*, 57, 1596  
Lecacheux, A., Biver, N., Crovisier, J., et al. 2003, *A&A*, 402, L55  
Mäkinen, J. T. T., Silén, J., Schmidt, W., et al. 2001, *Icarus*, 152, 268  
Neufeld, D. A., Stauffer, J. R., Bergin, E. A., et al. 2000, *ApJ*, 539, L151  
Osip, D. J., Schleicher, D. G., & Millis, R. L. 1992, *Icarus*, 98, 115  
Pilbratt, G. L., Riedinger, J. R., Passvogel, T., et al. 2010, *A&A* in press  
Roelfsema, P., Helmich, F., Teyssier, D., & et al. 2010, *A&A* this issue  
Szutowicz, S., Królikowska, M., & Rickman, H. 2008, *A&A*, 490, 393

- 
- <sup>1</sup> Max-Planck-Institut für Sonnensystemforschung, 37191 Katlenburg-Lindau, Germany
  - <sup>2</sup> LESIA, Observatoire de Paris, 5 place Jules Janssen, 92195 Meudon, France
  - <sup>3</sup> California Institute of Technology, Pasadena, CA 91125, USA
  - <sup>4</sup> Space Research Centre, Polish Academy of Sciences, Warsaw, Poland
  - <sup>5</sup> DLR, German Aerospace Centre, Bonn-Oberkassel, Germany
  - <sup>6</sup> Institute d'Astrophysique et de Geophysique, Université de Liège, Belgium
  - <sup>7</sup> Rosetta Science Operations Centre, European Space Astronomy Centre, European Space Agency, Spain
  - <sup>8</sup> Instituto de Astrofísica de Andalucía (CSIC), Spain
  - <sup>9</sup> STFC Rutherford Appleton Laboratory, Harwell Innovation Campus, Didcot, OX11 0QX, UK
  - <sup>10</sup> Instituut voor Sterrenkunde, Katholieke Universiteit Leuven, Belgium
  - <sup>11</sup> Astronomy Department, University of Michigan, USA
  - <sup>12</sup> Laboratory of Molecular Astrophysics, CAB-CSIC, INTA, Spain
  - <sup>13</sup> Sterrenkundig Instituut Anton Pannekoek, University of Amsterdam, Science Park 904, 1098 Amsterdam, The Netherlands
  - <sup>14</sup> LERMA, Observatoire de Paris, France
  - <sup>15</sup> SRON Netherlands Institute for Space Research, Landleven 12, 9747 AD, Groningen, The Netherlands
  - <sup>16</sup> Leiden Observatory, University of Leiden, The Netherlands
  - <sup>17</sup> Joint ALMA Observatory, Chile
  - <sup>18</sup> *Herschel* Science Centre, European Space Astronomy Centre, European Space Agency, Spain
  - <sup>19</sup> Department of Physics and Astronomy, University of Lethbridge, Canada
  - <sup>20</sup> KOSMA, I. Physik. Institut, Universität zu Köln, Zùlpicher Str. 77, D 50937 Köln, Germany
  - <sup>21</sup> Physikalisches Institut, University of Bern, Switzerland
  - <sup>22</sup> N. Copernicus Astronomical Center, Rabianska 8, 87-100, Torun, Poland
  - <sup>23</sup> Istituto Fisica Spazio Interplanetario-INAF, Via Fosso del Cavaliere 100, 00133 Roma, Italy
  - <sup>24</sup> Max-Planck-Institut für Radioastronomie, Auf dem Hügel 69, 53121 Bonn, Germany

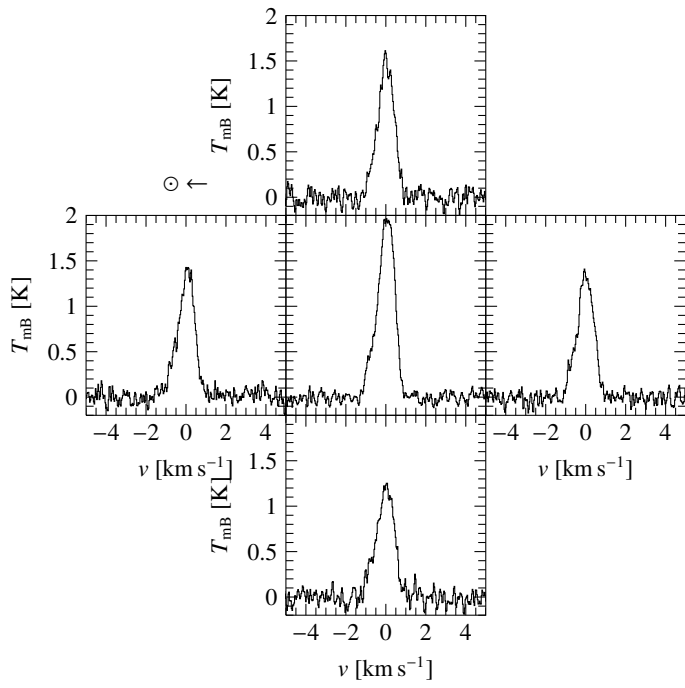


**Fig. 5.** DBS cross-map of the  $1_{10-1_{01}}$  ortho-water line obtained with the HRS on February 4.24 UT. The offset spacing is  $\sim 19''$  and the velocity resolution is  $\sim 32$  m s<sup>-1</sup>. The Sun direction is indicated.